TISSUE ENGINEERING: Part A
Volume 21, Numbers 1 and 2, 2015

DOI: 10.1089/ten.tea.2014.0028

Combination of BMP2 and MSCs Significantly Increases Bone Formation in the Rat Arterio-Venous Loop Model

Gregor Buehrer, MD,[1] Amelie Balzer, VMD,[1] Isabel Arnold, MD,[1] Justus P. Beier, MD,[1] Carolin Koerner, PhD,[2] Oliver Bleiziffer, MD,[1] Andreas Brandl, PhD,[1] Christian Weis, PhD,[3] Raymund E. Horch, MD,[1] Ulrich Kneser, MD,[1,4] and Andreas Arkudas, MD[1]

Introduction: In this study the induction of bone formation in an axially vascularized bone matrix using mesenchymal stem cells (MSCs) and application of bone morphogenetic protein 2 (BMP2) was analyzed in the arteriovenous loop (AVL) model.
Materials and Methods: An AVL was created in the medial thigh of 42 rats and placed in a porous titanium chamber filled with a particulated porous hydroxyapatite and beta-tricalcium phosphate matrix and fibrin. In group A the fibrin was loaded with 5×10^6 DiI-stained fibrin gel-immobilized primary MSCs from syngenic Lewis rats, in group B the matrix was loaded with 60 μg/mL BMP2 and in group C both, BMP2 and MSCs were applied at implantation time point. After 6 and 12 weeks, specimens were investigated by means of histological, morphometrical, and micro-computed tomography analysis.
Results: After implantation of an AVL a dense vascular network was visible in all groups. In group A, newly generated bone islands were detected in the periphery of the main vascular axis. Using BMP2 alone (group B), small islands of newly formed bone were visible evenly distributed in all parts of the constructs. In group C nearly the whole matrix was interspersed with bone formations. In all groups there was an increase of bone formation between the 6 and 12 weeks explantation time points.
Conclusions: This study demonstrates for the first time the successful generation of axially vascularized bone substitutes using MSCs and BMP2 in the AVL rat model using a one step procedure. Using the combination of BMP2 and MSCs there was a significant increase of bone formations detectable compared to the BMP2 or MSCs alone groups.

Introduction

Large bone defects can occur after trauma, tumor resection, avascular bone necrosis, or infections. Reconstruction of these bone defects is still challenging for any orthopedic or plastic surgeon because of the limited available bone substitutes. In areas of compromised vascularization after radiation, trauma, or infection, bone defects are clinically treated by transplantation of vascularized bone grafts from unharmed areas of the body including scapula, fibula, or iliac crest.[1] These procedures are associated with considerable donor site morbidity such as pain, hematoma, paresthesia, or reduction of function. In addition, these bone grafts are limited in shape and quantity.

Bone tissue engineering has emerged over the last decades and is intended to create bone grafts by the combination of a suitable biomaterial along with osteogenic cells and/or specific growth factors. Most tissue engineering studies are performed *in vitro* and bone generation has become a feasible challenge. Problems occur when *in vitro* approaches are transferred to *in vivo* mainly because of sometimes unforeseeable interactions with the body. Nowadays, one of the main problems of most *in vivo* tissue engineering approaches is the insufficient initial vascularization of implanted constructs. Vascularization can be achieved by either an extrinsic or intrinsic vascular pathway. In the past, numerous different animal models addressing an extrinsic type of vascularization such as the subcutaneous implantation model have been

Parts of this work have been presented at the 33rd Congress of German Society for Microsurgery of Peripheral Nerves and Vessels (2011, Vienna, Austria) and at the 3rd International Conference ''Strategies in Tissue Engineering'' (2012, Würzburg, Germany).
[1]Department of Plastic and Hand Surgery, University Hospital of Erlangen, Friedrich-Alexander-University of Erlangen-Nuernberg, Erlangen, Germany.
[2]Institute of Science and Technology of Metals and [3]Center for Medical Physics and Technology, Friedrich-Alexander-University of Erlangen-Nuernberg, Erlangen, Germany.
[4]Department of Hand, Plastic and Reconstructive Surgery, Burn Center, BG Trauma Center Ludwigshafen, University of Heidelberg, Heidelberg, Germany.

described. These concepts have proved their efficacy in extrinsically vascularized tissue engineered bone constructs but a microsurgical transfer of these specimens to the bone defect site remained impossible. Therefore, animal models with a defined vascular axis have been developed to overcome this problem. One of these models of intrinsic vascularization is the arteriovenous loop (AVL) model, which was first described by Erol and Spira in 1979.[2] Using this model, different clinically approved bone tissue engineering biomaterials such as processed bovine cancellous bone or a particulated hydroxyapatite and beta-tricalcium phosphate (HA/β-TCP) matrix have been axially vascularized over the last decade by our group.[3] To reduce the time interval between AVL implantation and transplantation into the defect site and to reduce surgical interventions, enhancement of vascularization was achieved by the combination of extrinsic and intrinsic vascular pathways by using newly developed custom made porous titanium chambers.[4] We were able to demonstrate that both vascular pathways connect as a mandatory requirement for further transplantation using the vascular pedicle of the AVL.

Osteogenic growth factors such as bone morphogenetic proteins (BMPs), transforming growth factor-β, and basic fibroblast growth factor have been described for bone tissue engineering purposes. Among them, BMP2 has been well characterized and is known as a potent osteoinductive protein.[5–7] We recently evaluated different concentrations of BMP2 and different growth factor release systems in a subcutaneous rat model in combination with different biomaterials.

Mesenchymal stem cells (MSCs) are pluripotent and can differentiate into multiple lineages such as osteocytes and chondrocytes and neural cells and myoblasts.[8] Osteogenic differentiated MSCs have been already widely used in bone tissue engineering approaches. To increase their osteogenic potential MSCs have been combined with osteogenic growth factors such as BMP2.[9]

The purpose of this study was to determine the optimal scaffold composition using MSCs as effector cells or rhBMP2 or the combination of MSCs and rhBMP2 with regard to bone generation and determine the ideal time point for free transplantation of the axially vascularized bone constructs.

Materials and Methods

Experimental design

All experiments were approved by the Animal Care Committee of the University of Erlangen and the Government of Mittelfranken, Germany (54-2532.1-24/09). Forty-two male Lewis rats (Charles River Laboratories) with a body weight of 200–230 g were operated. All operations were performed under sterile conditions by the same microsurgeon (A. Balzer) using an operating microscope (Karl Zeiss). All animals were randomly assigned to three different experimental groups: MSC only (group A), BMP2 only (group B), and the combination of MSC and BMP2 (group C).

An AVL was created in the left thigh of each animal as described previously.[10] Briefly, animals were operated under general anesthesia using isoflurane (Baxter). First, the left femoral vessels were isolated and a vein graft of the right femoral vein was microsurgically interposed between the left artery and vein, creating an AVL. Afterwards, the AVL was embedded into a clinically approved granular porous hydroxyapatite and beta-tricalcium phosphate (60% HA and 40% β-TCP, particle size 1–2 mm, micro-porosity < 10 μm, macro-porosity 300–600 μm, TricOs®; Baxter Healthcare S.A.) matrix and fibrin gel (Tisseel VH S/D; Baxter Healthcare S.A.) with a final fibrinogen concentration of 10 mg/mL and a final thrombin concentration of 2 IU/mL (Fig. 1). Also, aprotinin was added with a final concentration of 1500 KIE/mL to delay fibrinolysis. The construct was placed within a porous titanium chamber with an inner diameter of 10 mm and a height of also 10 mm, made of Ti-6Al-4V by selective electron beam melting (C. Koerner, Institute of Science and Technology of Metals, University of Erlangen-Nuernberg, Germany). The pore sizes of the chamber were 1–2 mm. The fibrin gel was loaded prior implantation with 5×10^6 MSCs in group A, 60 μg/mL recombinant human BMP2 (R&D Systems) in group B, or 60 μg/mL BMP2 and 5×10^6 MSCs in group C.

At 6 and 12 weeks postoperatively, constructs were harvested and *ex vivo* high resolution micro-computed tomography (micro-CT) scans were obtained of one specimen per group and explantation time point. Afterwards, all constructs were analyzed for histological and immunohistochemical properties.

MSC isolation

MSCs were isolated based on plastic adherence. Briefly, MSCs were derived from the femoral and tibial bone marrow of male Lewis rats after sacrificing the animals using CO_2 asphyxiation. Afterwards, bone marrow plugs were hydrostatically expelled and disaggregated with a needle and a syringe. Cells were placed in flasks filled with Dulbecco's modified Eagle's medium (Gibco Invitrogen) with 20% fetal bovine serum (Lot.No. 934 FF; Biochrom AG), 1% penicillin/streptomycin (Gibco Invitrogen), and 1% L-glutamin (Sigma-Aldrich). The cell suspension was cultured until confluence. After 72 h, the medium was completely replaced to remove all unattached hematopoietic cells. Adherent cells were expanded as monolayer cultures in a humidified atmosphere of 5% CO_2 and 95% air at 37°C. Afterward, the medium was changed twice weekly until cells reached 80% confluence in a flask. Then, cells were trypsinized and cultured further until passage 5. The cells were osteogenically differentiated 5 days prior to implantation using differentiation medium (25 mg/L L-ascorbat-2-

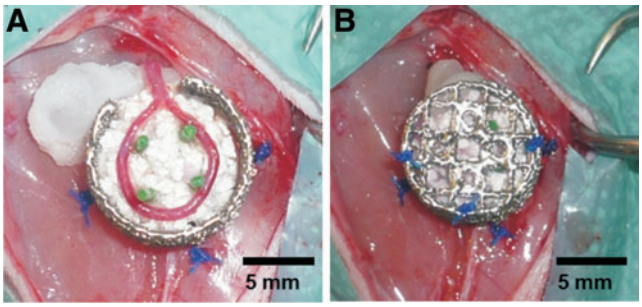

FIG. 1. Implantation of the arteriovenous loop (AVL). The AVL was placed on the first half of the matrix **(A)**. Afterwards, the chamber was filled with the second half of the matrix and the lid was closed **(B)**. Color images available online at www.liebertpub.com/tea

phosphat, 10 mM β-glycerol-2-phosphat, and 100 nM dexamethason [water-soluble; all from Sigma-Aldrich]; added to regular cell culture medium). Before cell implantation cells were labeled with DiI (Cell Tracker TM CM-DiI; Invitrogen).

Explantation procedures

Six and 12 weeks after the AVL implantation India ink or Microfil® perfusion was performed to determine vascularization of matrizes. First, the descending aorta was canulated, the inferior caval vein cut and the vascular system was flushed with Ringer-heparin (100 IU/mL) solution until the leaking fluid was clear. Five animals from each group were perfused with 20 mL India ink (50% v/v India ink [Rohrer] in 5% gelatine [Roth] and 4% mannitol [Neolab]) and one animal per group was perfused with 20 mL of Microfil® solution (Microfil MV-122, containing 0.6 mL of curing agent; Flow Tech). Finally, the aorta and inferior caval vein were ligated and the rats were placed at 4°C overnight. Afterwards, constructs were explanted, fixed in 3.5% formalin solution, and decalcified in ethylenediaminetetraacetic acid (EDTA; Sigma-Aldrich Chemie GmbH) for 3 weeks at 4°C. One Microfil perfused construct per group and explantation time point was prepared for micro-CT analysis, whereas all India ink-perfused scaffolds were processed for histological analysis.

Histological analysis

After explantation constructs were macroscopically inspected, weighed, decalcified in EDTA, and embedded in paraffin. Three micrometers cross sections were obtained from two standardized planes perpendicular to the longitudinal axis of the AVL using a microtome (Leica Microsystems).

Cross sections were stained with hematoxylin and eosin (H&E) and Masson's trichrome according to standard protocols. All cross sections were photographed using a Leica microscope (Carl Zeiss) and a digital camera under 25× magnification and subsequently merged to one image. Bone areas within each specimen were semiautomatically measured using Leica Application Suite V3 (Leica Microsystems).

Automatic quantitative evaluation of vascularization

The evaluation is based on the ''negative- and positive-experts''-model[11] and on the (corrected) nearest-neighbor-classification/k-means-clustering[12] applied on microscopy images of histological cross sections. The program was written in MATLAB using the image processing toolbox and the statistics toolbox. A precise description of this approach can be found in previous studies.

Multiple brightfield images of stained histological cross sections were acquired at a four fold magnification with an inverse microscope (IX81; Olympus) equipped with a digital camera (SC30; Olympus). Imaging was controlled by the cellSens Dimension V1.5 (Olympus) software. To cover the whole sample all acquired images were merged within cellSens with the multiple image acquisition functionality.

To identify the colored vessels on histologic slides, negative experts (sample background, dark objects, such as nuclei of H&E- and lectin-staining, etc.) and positive experts (vessels) were generated. The images were then transformed from the conventional RGB color space to the CIELAB color space. In this color space a model was trained based on the previously defined experts. Afterward, all pixels of the image were classified according to the model. The result is saved as a binary map, showing the pixels' classification as ''pixels containing vessels'' and ''pixels not containing vessels''. Then, the main vessels were marked and each segmented vessel was assigned to the nearest main vessel. During this assignment vessels were transformed from the image domain to a vector-based geometric two-dimensional representation (only consisting of the vessel's center and its radius). This transformation is necessary for the calculations of statistics such as number and area of vessels depending on the distance to the main vessels, and their classification in ''next to the main vessels'' and ''next to the sample's periphery''.

Immunohistology

Endothelial cells were identified using the lectin Bandeiraea Simplicifolia agglutinin (BS-1) as described elsewhere.[10] Briefly, detection was performed with a biotinylated lectin (BS-1, 1:100 dilution; Sigma) overnight at 4°C, followed by a streptavidin AB complex/HRP (Dako GmbH) for 30 min and DAB + chromogen (Dako GmbH).

Macrophages were detected using ED1 immunostainings as described previously.[10] Identification was carried out using a 1:300 anti-ED1 primary antibody (Serotec), followed by a goat anti-mouse secondary antibody (Dako GmbH) at a concentration of 1:20 (30 min). Sections were subsequently incubated with 1:50 APAAP complex (alkaline phosphatase–anti-alkaline phosphatase) (30 min).

To detect smooth muscle cells, sections were stained using alpha-smooth muscle actin (ASMA) as described elsewhere.[10] Therefore, sections were incubated with a 1:300 mouse anti-ASMA primary antibody (Dako GmbH), followed by an anti-mouse anti-rabbit secondary antibody (Invitrogen).

Apoptotic cells were identified using a TUNEL assay (FragEL™ DNA Fragmentation Detection Kit; Calbiochem).

Real-time polymerase chain reaction

Total RNA from all paraffin-embedded cross sections of the central part of the constructs was isolated using theRNeasy FFPE Kit (Qiagen) according to the manufacturer's instructions. One microgram RNA was reversely transcribed into cDNA using the RevertAid First Strand cDNA Synthesis Kit (Thermo Fischer Scientific, Inc.). The amount of each target transcript was normalized to GAPDH respectively. The calculation of the expression ratios was performed using the comparative Ct-method. The polymerase chain reaction (PCR) run was performed in a CFX96 Touch™ Real-Time PCR Detection System and analyzed with the CFX Manager™ Software (Bio-Rad Laboratories, Inc.). Primers used for PCR: VEGF_for:AATGATGAAGCC CTGGAGTG; VEGF_rev: ATGCTGCAGGAAGCTCATCT; RUNX2_for: CCACCACTCACTACCACACG; RUNX2_rev: TATGGAGTGCTGCTGGTCTG; Osteocalcin_for: CATGAG GACCCTCTCTCTGC; Osteocalcin_rev: TTCACCAACCTT ACTGCCTC; Osteopontin_for: GATCGATAGTGCCGAGA AGC; Osteopontin_rev: TGAAACTCGTGGCTCTGATG; GA

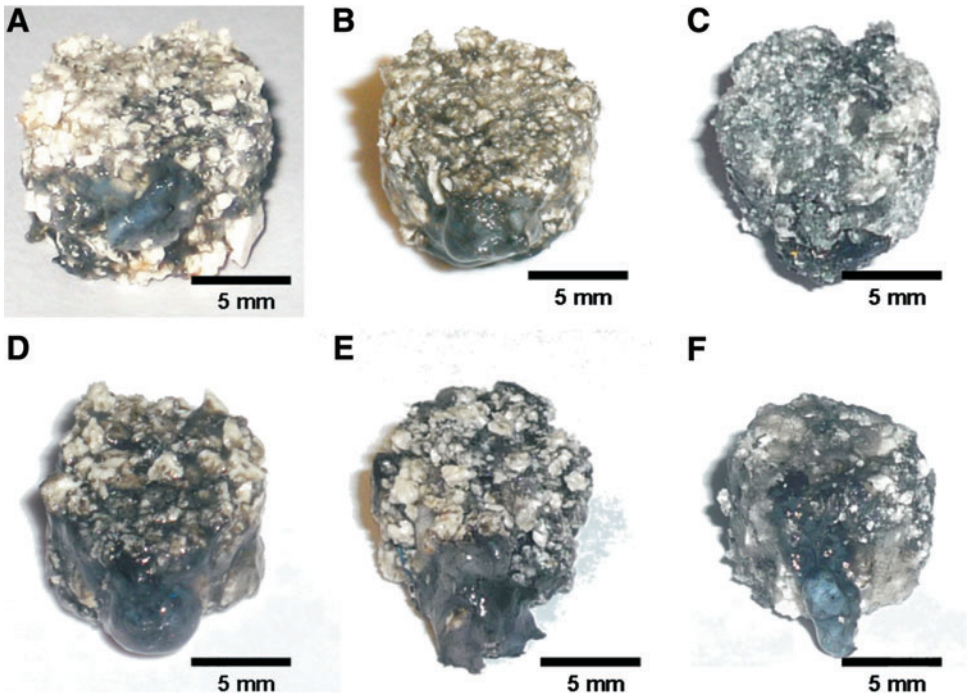

FIG. 2. Macroscopic appearance of the constructs. Vascularization of all constructs was macroscopically evident in the surroundings and the AVL by black (India ink) filling of vessels with no macroscopic difference between all groups and explantation time points. Also, no degradation of constructs was detectable at all explantation time points. **(A–C)** Six weeks explantation time point; **(D–F)** 12 weeks explantation time point; **(A, D)** group A; **(B, E)** group B; **(C, F)** group C. Color images available online at www.liebertpub.com/tea

PDH_for: AATGCATCCTGCACCACCAACT; GAPDH_rev: ATCCACAGTCTTCTGAGTGGCAGT.

Micro-computed tomography

One construct per group and explantation time point was investigated using micro-CT. These animals were then perfused with yellow Microfil® as described previously.[3] Explanted and decalcified constructs were analyzed using a micro-CT scanner (μCT40; Scanco Medical) with the following scanning parameters: tube voltage 40 kV, 180 μA, 15 μm voxel size.

Statistical analysis

Data were expressed as mean ± standard deviation. Statistical analysis was performed using GraphPad Prism (GraphPad Software, Inc.). One-way analysis of variance and student *t*-tests were applied for statistical analysis. The critical level of statistical significance chosen was $p < 0.05$.

Results

Surgical procedures and macroscopic appearance

All 42 animals tolerated the surgical procedures and the implanted chambers without major complications such as infections, hematomas, or dislocations. Upon explantation, two AVLs showed signs of thrombosis and were excluded from further evaluation. All titanium chambers were encapsulated with fibrous tissue at the explantation time points. At harvest the titanium chambers showed a tight integration in the newly formed bone constructs; thus, removal of the chambers appeared to be difficult. Bone density appeared higher at gross examination in group C compared with groups A and B at 6 weeks explantation time point with no further increase in all groups until the 12 weeks explantation time point. There were no signs of degradation or resorption in all groups (Fig. 2). At 6 weeks explantation time point mean construct weights of all groups showed no significant difference (group A: 0.96 ± 0.05 g; group B: 0.92 ± 0.04 g; and group C: 1.01 ± 0.14 g). At 12 weeks constructs of group C demonstrated a significantly increased construct weight compared with groups A and B (group A: 0.98 ± 0.04 g; group B: 0.91 ± 0.06 g; and group C: 1.25 ± 0.08 g). Also constructs of group C showed a significantly increased construct weight between both explantation time points, whereas the mean construct weights of groups A and B did not significantly differ over time.

Vascularization of all constructs was macroscopically evident in the surroundings and the AVL by black (India ink) or yellow (Microfil®) filling of vessels with no macroscopic difference between all groups and explantation time points.

Micro-computed tomography

Vascularization of one specimen per group and time point was quantitatively visualized using micro-CT. These images showed a dense vascular network throughout the constructs (Fig. 3). There were no AVL thromboses detectable in the micro-CTs of all scanned constructs. All specimens showed extrinsic vessels entering the chambers from the periphery and sprouts emerging from the AVL forming the intrinsic part of the vascular network.

Histological evaluation

Histological analysis confirmed that at 6 and 12 weeks the fibrin gel part of the matrix in all groups was completely degraded and replaced by highly vascularized newly formed connective tissue, whereas the β-TCP/HA granules showed

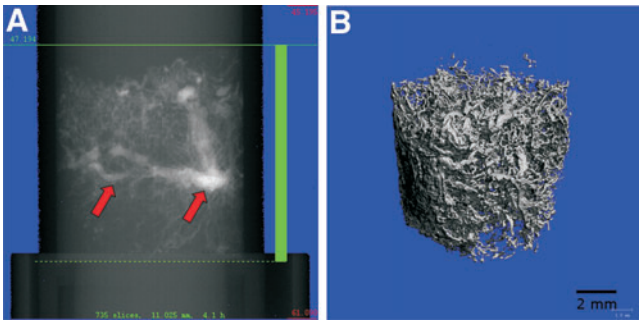

FIG. 3. Micro-computed tomography of the vascular network within the specimen 6 weeks after implantation before **(A)** and after **(B)** reconstruction (*arrows:* AVL). Color images available online at www.liebertpub.com/tea

no signs of degradation or resorption. Functional vessels could be detected in the histological sections by black filling of lumina with India ink. Endothelial cells were detected by lectin immunostainings. Vitality of MSCs was demonstrated by diamidine-phenylindole-dihydrochloride (DAPI) staining in all specimens, although the number of viable cells differed between the constructs. In both groups A and C the total number of MSCs decreased over time between the 6 and 12 weeks explantation time point.

Morphometric evaluation of the cross-sectional area revealed a significantly increased cross-sectional area at 6 weeks in group C compared with the other groups at the same explantation time point (group A: $43.09 \pm 6.27\,mm^2$; group B: $40.36 \pm 9.27\,mm^2$; and group C: $54.85 \pm 11.44\,mm^2$). At 12 weeks explantation time point constructs of group C were found to be significantly larger than those in groups A and B (group A: $37.77 \pm 5.59\,mm^2$; group B: $42.86 \pm 5.68\,mm^2$; and group C: $66.1 \pm 3.75\,mm^2$). Furthermore, there was a significant increase of cross-sectional area in group C over time, whereas construct areas of groups A and B showed no significant differences between the two time points.

Histological evaluation of bone formation

H&E and Masson's trichrome stainings revealed bone formations on all cross sections. In addition to bone generation, the complete newly formed tissue within the granules of the HA/β-TCP matrix was composed of inflammatory cells, fibroblasts, blood vessels, and vascular sprouts. The newly generated bone formations were located close to the β-TCP/HA granules and were in particular evident in vascularized parts of the construct. Osteoblastic and osteoclastic processes were detected in the newly formed bone, revealing an active bone remodeling process. The implanted MSCs were detected due to their DiI labeling prior to implantation. Sections were also counterstained with DAPI (Roche Diagnostics GmbH). Vital MSCs were detected in close proximity to the bone formations and in the connective tissue. Bone formation showed different patterns of distribution in groups A–C. In group A, newly formed bone was exclusively located in the surrounding of the AVL vessels, whereas in group B, small bone formations were distributed over the complete specimen without larger accumulations (Figs. 4 and 5). In group C, nearly the complete space between the β-TCP/HA granules was filled with newly generated bone formations. There was the same pattern of distribution detectable in all groups at the 6 and 12 weeks explantation time points.

Morphometric evaluation of bone formation revealed a significant increase of the total area of bone formation at 6 and 12 weeks between group C and groups B and A (group A—6 weeks: $0.03 \pm 0.09\,mm^2$; group B—6 weeks: $0.84 \pm 0.5\,mm^2$; and group C—6 weeks: $9.18 \pm 5.3\,mm^2$; group A—12 weeks: $0.86 \pm 0.64\,mm^2$ group B—12 weeks: $1.65 \pm 0.7\,mm^2$; and group C—12 weeks: $14.34 \pm 2.86\,mm^2$).

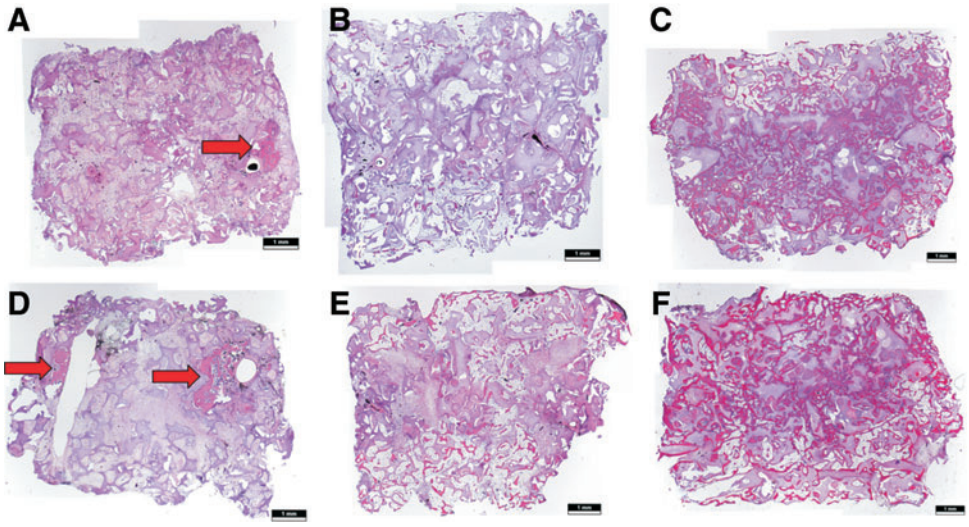

FIG. 4. H&E stainings revealed bone formations on all cross sections. Bone formation showed different patterns of distribution regarding groups A–C. In group A, newly formed bone was located in the surrounding of the AVL vessels (arrows), whereas in group B small bone regions were distributed over the complete specimen without larger accumulations. In group C, nearly the whole constructs were filled with newly formed bone. **(A–C)** Six weeks explantation time point; **(D–F)** 12 weeks explantation time point; **(A, D)** group A; **(B, E)** group B; **(C, F)** group C. H&E, hematoxylin and eosin. Color images available online at www.liebertpub.com/tea

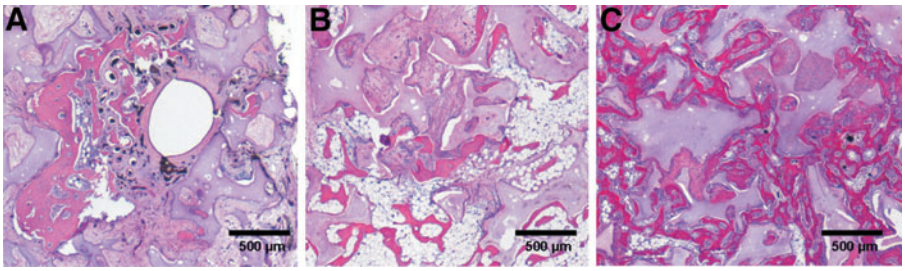

FIG. 5. Selected details of Figure 4D–F: The newly generated bone was located in proximity to the β-TCP/HA granules and were, in particular, evident in vascularized parts of the construct. **(A)** Group A; **(B)** group B; **(C)** group C. Twelve weeks explantation time point. Color images available online at www.liebertpub.com/tea

Furthermore all groups displayed a significant increase of bone formation area between the 6 and 12 weeks explantation time points ($p < 0.05$).

Morphometric evaluation of the mean bone formation proportion was similar compared with the total bone area evaluation (Fig. 6). The mean bone area proportion at 6 and 12 weeks was significantly increased in group C compared with group B and group A (group A—6 weeks: 0.05% ± 0.19%; group B—6 weeks: 2.02% ± 1.06%; and group C—6 weeks: 16.08% ± 7.3%; group A—12 weeks: 2.2% ± 1.6%; group B—12 weeks: 3.87% ± 1.64%; and group C—12 weeks: 21.63% ± 3.74%). There was also an increase of bone formation proportion in all groups over time.

Automatic quantitative evaluation of vascularization

Automatic assessment of vascularization pattern inside the constructs was feasible. At 6 weeks there were significantly more vessels detectable in the periphery compared with the central part of the construct in group B (158.50 ± 122.27 vs. 59.70 ± 46.11 vessels/cross section) and in group C (228.42 ± 114.13 vs. 86.25 ± 46.60 vessels/cross section). At 12 weeks in group A and B significantly more vessels were detected in the periphery compared with the central part of the construct (group A: 224.60 ± 112.92 vs. 107.60 ± 76.23 vessels/cross section and group B: 260.42 ± 139.45 vs. 83.42 ± 45.65 vessels/cross section). At 6 weeks there were significantly more vessels detectable in group A compared with group B (548.5 ± 332.91 vs. 218.2 ± 166.43 vessels/cross section) (Fig. 7). There were no significant differences detectable between group C and the other two groups after 6 weeks. After 12 weeks group C displayed a significantly deceased total vessel number per cross section compared with groups A and B after 12 weeks (80.42 ± 86.85 [group C] vs. 332.2 ± 169.35 [group A] vs. 343.83 ± 179.81 [group B] vessels/cross section). There was also a significant decrease of the total vessel count detectable in group C between the 6 and 12 weeks explantation time point.

Real-time PCR

Gene expression profiles for scaffolds are shown in Figure 8. The relative expressions of alkaline phophatase (ALP), osteocalcin, osteopontin, runx2, and VEGF were increased in group C compared with groups A and B after 6 weeks. At 12 weeks the relative expression of OC and runx2 was still increased compared with groups A and B, whereas VEGF expression decreased in group C after 12 weeks.

Discussion

Bone tissue engineering represents a research field aimed to generate artificial bone grafts that could be used as a replacement for autologous bone transplants in reconstructive and orthopedic surgery.[13] Despite the broad spectrum of biomaterials, cells and signal molecules, tissue engineering techniques have not yet reached clinical application. Currently, vascularized autologous bone grafts represent the gold standard for treatment of large osseus defects in clinical practice. However, the harvest of these grafts has several disadvantages like donor site morbidity or limitations regarding size and shape of the bone grafts.[14]

In this study, we used the AVL model to generate axially vascularized bone constructs first described by Erol and

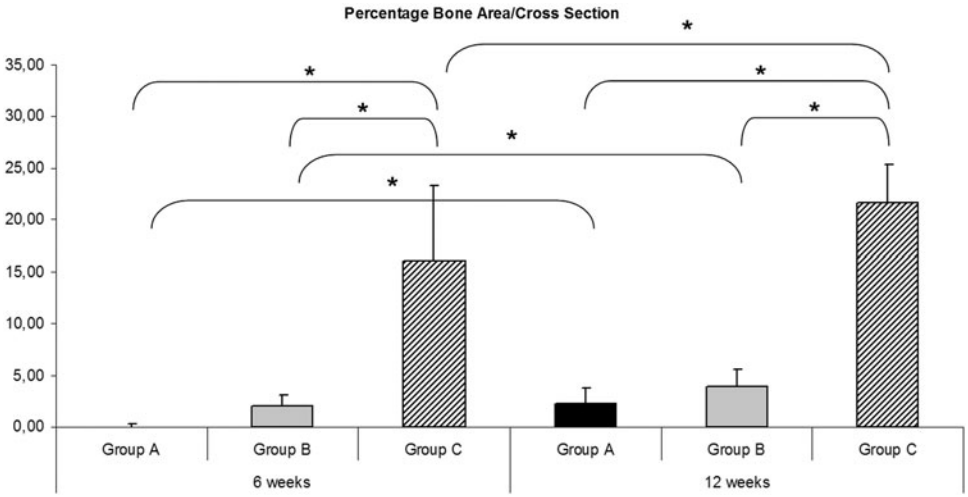

FIG. 6. Morphometric evaluation of the mean bone formation proportion was similar compared to the total bone area evaluation. The mean bone area proportion at 6 and 12 weeks was significantly (*) increased in group C compared with group B and group A. There was also an increase of bone formation proportion in all groups over time ($p < 0.05$).

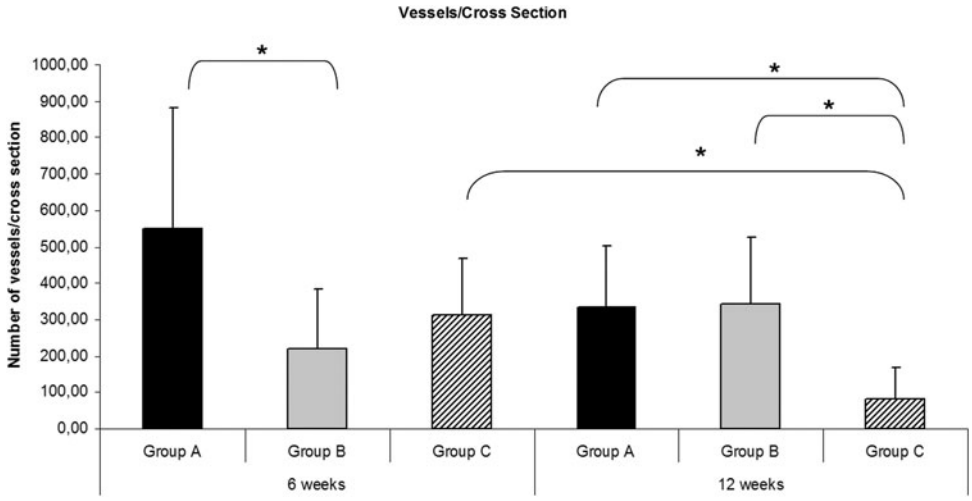

FIG. 7. Automatic assessment of total number of vessels per cross section. At 6 weeks there were significantly more vessels detectable in group A compared with group B. After 12 weeks group C displayed a significantly (*) decreased total vessel number per cross section compared with groups A and B after 12 weeks. There was also a significant decrease of the total vessel count detectable in group C between the 6 and 12 weeks explantation time point ($p < 0.05$).

Spira in 1979 and further augmented by Morrison and coworkers.[2,15,16] Our group has previously studied the combination with an additional extrinsic vascular pathway by using newly developed custom-made porous titanium chambers.[4] We were able to show that both vascular networks connect already after 2 weeks of implantation allowing transplantation of the whole vascular system using the AVL pedicle.

In this study, we used diluted fibrin with a fibrinogen concentration of 20 mg/mL and a thrombin concentration of 4 IU/mL as the release system for BMP2 based on previous subcutaneous studies comparing this BMP2 release system with undiluted fibrin, collagen sponge, and heparin-conjugated fibrin (HCF). Although Yang *et al.* were able to show a prolonged release period of BMP2 *in vitro* and an increased *in vivo* bone generation using HCF immobilized BMP2 compared to collagen sponges, we were not able to verify these observations in our *in vivo* subcutaneous model.[17,18]

With respect to bone generation, we used a BMP2 concentration of 60 μg/mL in this study. Clinically, the current FDA-approved BMP2 concentration is 1.5 mg/mL often combined with collagen sponges as the release system. Recently, Zara *et al.* were able to test different BMP2 concentrations ranging from 5 to 600 μg/mL in a segmental femoral defect model in rat.[19] Their findings demonstrated that BMP2 concentrations higher than 30 μg/mL lead to bony unions, whereas high BMP2 concentrations of 150–600 μg/mL did not improve bone healing and promoted the generation of cyst-like bony shells. In prestudies, we evaluated different concentrations of BMP2 in the granular porous hydroxyapatite and beta-tricalcium phosphate matrix used in this study. We found out that the minimum dose of BMP2 to induce consistent bone formations in the subcutaneous rat model was 60 μg/mL, whereas lower doses ranging from 2.5 to 12.5 μg/mL did not produce osteoinductive effects. Higher BMP2 concentrations up to 700 μg/mL did not contribute to an increased bone generation; therefore, a BMP2 concentration of 60 μg/mL was used in this study.

We used the clinically approved granular porous hydroxyapatite and beta-tricalcium phosphate matrix based on the following considerations: beside the proven bone generation in the subcutaneous model using BMP2 alone we were able to axially vascularize the HA/β-TCP matrix in the AVL model in previous studies.[3,4] HA can also serve as a release system for BMP2 because of its strong binding

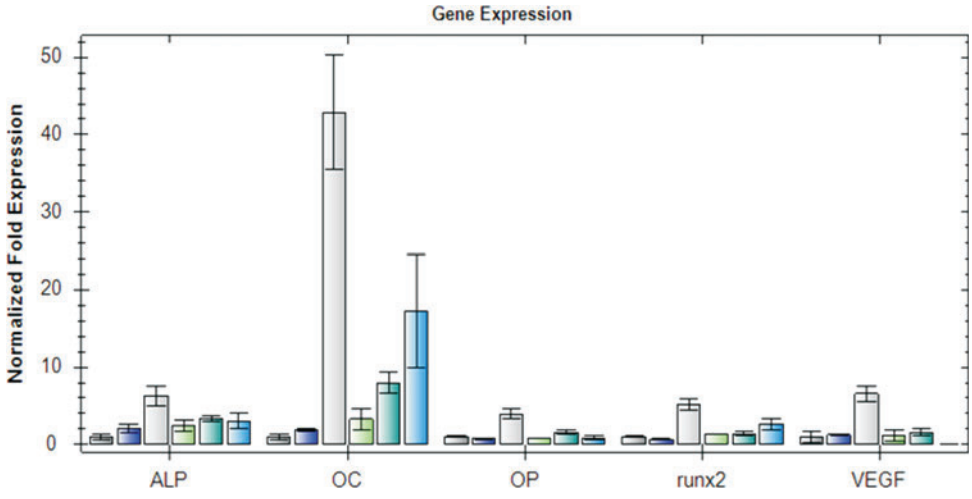

FIG. 8. Real-time polymerase chain reaction. The relative expressions of ALP, osteocalcin, osteopontin, runx2, and VEGF were increased in group C compared with groups A and B after 6 weeks. At 12 weeks, the relative expression of OC and runx2 was still increased compared with groups A and B, whereas VEGF expression decreased in group C after 12 weeks (from left to right: 6 weeks groups A–C, 12 weeks groups A–C). ALP, alkaline phophatase. Color images available online at www.liebertpub.com/tea

affinity.[20,21] The slow release kinetic can also be attributed to the low bioresorbability of HA, whereas β-TCPs are completely degraded during bone generation. Seebach *et al.* recently demonstrated that MSCs adhere to β-TCP, although their surface structure essentially influenced the cell seeding.[22] In this study, there was no degradation of the HA/β-TCP matrix detectable, maybe because of the explantation time points of 6 and 12 weeks and the high amount of HA. As expected the fibrin gel was disintegrated and replaced with vascularized connective tissue after 6 weeks.

Newly formed bone was predominately located in proximity to the matrix granules in all groups and explantation time points. Histological analysis revealed that bone formation within the MSC group A predominantly took place in the vicinity of the AVL. In contrast, the group B with BMP2 showed generalized bone formation, even in the central parts of the construct. This shows that osteogenically differentiated MSCs or BMP2 on its own are capable of forming bone tissue in this model. Thinking on the mechanisms behind these different patterns of bone formation, vascularization of these constructs plays a crucial role. In this study, we used a one step procedure including AVL creation and MSC implantation. Newly formed bone in group A is strongly related to the presence of vital MSCs because in previous studies using the same matrix and animal model we were unable to detect bone formations without application of either MSCs or BMP2 up to an explantation time point of 8 weeks.[3] Vascularization of matrices first takes place in the proximity of the AVL or in the surrounding of the specimens representing the extrinsic type of vascularization because of the porous chambers. The time frame necessary for the matrix vascularization is critical for any cell containing *in vivo* study, in particular when no prevascularization period prior to the cell injection is included. The evenly distributed bone formation of specimens in group B is most likely because of the evenly distributed BMP2 in the entire specimens leading to osteogenic differentiation of pluripotent cells of the host organism and migration to bone formation sites. It could be speculated that the vascularization of the scaffolds comes along with the proceeding migration of host cells because cells can only survive within a maximum range of 200 μm through diffusion.[23]

In this study, there was a significant increase of bone formation detectable in group C by the combination of MSCs and BMP2 compared with groups A and B. MSCs appeared superior to other cell sources in previous studies regarding osteoinduction and osteogenic differentiation.[13,24] The influence of BMP2 on the osteogenic differentiation of MSCs is already well known. Na *et al.* were able to show an increased osteogenic differentiation of MSCs after implantation into three-dimensional hybrid scaffolds containing HA, poly(NiPAAm-co-AAc) and BMP2.[25] Stephan *et al.* combined an injectable biopolymer of chitosan and inorganic phosphates with MSCs, BMP2, or both MSC and BMP2 and observed the bone generation in a rat calvarial critical size defect model.[26] Similar to our study, the MSC/BMP2 group showed an enhanced bone formation compared with the other two groups. Boos *et al.* evaluated directly autotransplanted MSCs with and without BMP2 application in the sheep AVL model.[9] They were able to demonstrate an increased amount of bone formation in the MSC/BMP2 group compared with the group without osteogenic growth factor application. Strobel *et al.* investigated novel biphasic calcium phosphate matrices containing osteoblasts and/or BMP2 in the subcutaneous rat model.[27] Scaffolds containing the combination of osteoblasts and BMP2 showed superior bone generation compared with the other groups *in vivo*. The osteogenic effect of BMP2 on the host cells like preosteoblasts or MSCs might be limited in group B with regard to the BMP2 release kinetics. In group C, the implanted BMP2 already effects the osteogenically differentiated MSCs starting at the implantation time point, which could explain the significant differences between groups B and C.

The porous chamber model has proven to be effective for combining extrinsic and intrinsic pathways of vascularization.[4] In this study, we used a novel automatic quantitative evaluation of vascularization pattern by determining the distance between the vessels and the AVL as the intrinsic vascular pathway and the outer scaffold border as the origin of the extrinsic vascularization. Using this technique, the vessel origins can only be estimated based on the measured distances because after 6 weeks most sprouts of the intrinsic and extrinsic vascular pathway have already been connected. Since the extrinsic vascular pathway can enter the scaffold at any location of the matrix surface compared to the very defined vascular axis of the AVL, the number of extrinsic vessels surpassed the intrinsic vessel count in all groups. We found out that in group C there was a significant decrease of vessel number detectable between the 6 and 12 weeks explantation time point and compared to groups A and B at 12 weeks, which was in concordance with the decreased VEGF expression in this group. This finding was possibly due to the increased bone formation in this group leading to a limited vascular network between the bone formations. Also, maturation of the vascular network in group C in terms of regression and persistence can cause the decreased vessel number in group C.

To our best knowledge this is the first study to produce axially and extrinsically vascularized bioartificial bone substitutes by combining MSCs, BMP2, and a HA/β-TCP scaffold in the AVL model of the rat. This study may provide the basis for further pedicled or free transplantation into a defect model to examine suitable surgical procedures and possible integration of the preformed bone constructs. Furthermore, upscaling of the described procedures and techniques into a large animal model using the porous titanium chamber is required before clinical application. In the future these results may have significant impact on clinical flap prefabrication purposes for bone defect reconstruction.

Conclusion

This study demonstrates for the first time the enhancement of bone formation by combining MSCs and BMP2 in the AVL model of the rat. Although each component, MSCs or BMP2 alone, lead to bone generation, the combination of both significantly enhanced the amount of generated bone.

In the future custom-made bone substitutes developed in this study by combining MSCs, BMP2 and an axially vascularized HA/β-TCP scaffold could probably be applied in a clinical scenario to overcome the inherent disadvantages of

autologeous bone substitutes such as donor site morbidity or limitations regarding size and shape.

Acknowledgments

This work contains parts of Gregor Buehrer's doctoral thesis. This study was supported by research grants from AO Research Fund Grant S-10-36A and Baxter Healthcare Corporation.

Disclosure Statement

No competing financial interests exist.

References

1. Beris, A.E., Lykissas, M.G., Korompilias, A.V., Vekris, M.D., Mitsionis, G.I., Malizos, K.N., and Soucacos, P.N. Vascularized fibula transfer for lower limb reconstruction. Microsurgery **31,** 205, 2011.
2. Erol, O.O., and Spira, M. New capillary bed formation with a surgically constructed arteriovenous fistula. Surg Forum **30,** 530, 1979.
3. Arkudas, A., Beier, J.P., Pryymachuk, G., Hoereth, T., Bleiziffer, O., Polykandriotis, E., Hess, A., Gulle, H., Horch, R.E., and Kneser, U. Automatic quantitative micro-computed tomography evaluation of angiogenesis in an axially vascularized tissue-engineered bone construct. Tissue Eng Part C Methods **16,** 1503, 2010.
4. Arkudas, A., Pryymachuk, G., Beier, J.P., Weigel, L., Korner, C., Singer, R.F., Bleiziffer, O., Polykandriotis, E., Horch, R.E., and Kneser, U. Combination of extrinsic and intrinsic pathways significantly accelerates axial vascularization of bioartificial tissues. Plast Reconstr Surg **129,** 55e, 2012.
5. Kim, J.W., Choi, K.H., Yun, J.H., Jung, U.W., Kim, C.S., Choi, S.H., and Cho, K.S. Bone formation of block and particulated biphasic calcium phosphate lyophilized with *Escherichia coli*-derived recombinant human bone morphogenetic protein 2 in rat calvarial defects. Oral Surg Oral Med Oral Pathol Oral Radiol Endod **112,** 298, 2011.
6. Lo, K.W., Ulery, B.D., Ashe, K.M., and Laurencin, C.T. Studies of bone morphogenetic protein-based surgical repair. Adv Drug Deliv Rev **64,** 1277, 2012.
7. Keibl, C., Fugl, A., Zanoni, G., Tangl, S., Wolbank, S., Redl, H., and van Griensven, M. Human adipose derived stem cells reduce callus volume upon BMP-2 administration in bone regeneration. Injury **42,** 814, 2011.
8. Pittenger, M.F., Mackay, A.M., Beck, S.C., Jaiswal, R.K., Douglas, R., Mosca, J.D., Moorman, M.A., Simonetti, D.W., Craig, S., and Marshak, D.R. Multilineage potential of adult human mesenchymal stem cells. Science **284,** 143, 1999.
9. Boos, A.M., Loew, J.S., Deschler, G., Arkudas, A., Bleiziffer, O., Gulle, H., Dragu, A., Kneser, U., Horch, R.E., and Beier, J.P. Directly auto-transplanted mesenchymal stem cells induce bone formation in a ceramic bone substitute in an ectopic sheep model. J Cell Mol Med **15,** 1364, 2012.
10. Arkudas, A., Pryymachuk, G., Hoereth, T., Beier, J.P., Polykandriotis, E., Bleiziffer, O., Horch, R.E., and Kneser, U. Dose-finding study of fibrin gel-immobilized vascular endothelial growth factor 165 and basic fibroblast growth factor in the arteriovenous loop rat model. Tissue Eng Part A **15,** 2501, 2009.
11. Kalal, Z., Matas, J., and Mikolajczyk, K. 2010 IEEE Computer Society Conference on Computer Vision and Pattern Recognition (CVPR). IEEE, 2010, pp. 49–56. http://ieeexplore.ieee.org/Xplore/home.jsp
12. Seber, G. Multivariate Observations. In: Wiley Series in Probability and Mathematical Statistics—Multivariate Analysis, Wiley, 1984.
13. Arvidson, K., Abdallah, B.M., Applegate, L.A., Baldini, N., Cenni, E., Gomez-Barrena, E., Granchi, D., Kassem, M., Konttinen, Y.T., Mustafa, K., Pioletti, D.P., Sillat, T., and Finne-Wistrand, A. Bone regeneration and stem cells. J Cell Mol Med **15,** 718, 2011.
14. Dimitriou, R., Jones, E., McGonagle, D., and Giannoudis, P.V. Bone regeneration: current concepts and future directions. BMC Med **9,** 66, 2011.
15. Lokmic, Z., Stillaert, F., Morrison, W.A., Thompson, E.W., and Mitchell, G.M. An arteriovenous loop in a protected space generates a permanent, highly vascular, tissue-engineered construct. FASEB J **21,** 511, 2007.
16. Lokmic, Z., Thomas, J.L., Morrison, W.A., Thompson, E.W., and Mitchell, G.M. An endogenously deposited fibrin scaffold determines construct size in the surgically created arteriovenous loop chamber model of tissue engineering. J Vasc Surg **48,** 974, 2008.
17. Yang, H.S., La, W.G., Bhang, S.H., Jeon, J.Y., Lee, J.H., and Kim, B.S. Heparin-conjugated fibrin as an injectable system for sustained delivery of bone morphogenetic protein-2. Tissue Eng Part A **16,** 1225, 2010.
18. Yang, H.S., La, W.G., Cho, Y.M., Shin, W., Yeo, G.D., and Kim, B.S. Comparison between heparin-conjugated fibrin and collagen sponge as bone morphogenetic protein-2 carriers for bone regeneration. Exp Mol Med **44,** 350, 2012.
19. Zara, J.N., Siu, R.K., Zhang, X., Shen, J., Ngo, R., Lee, M., Li, W., Chiang, M., Chung, J., Kwak, J., Wu, B.M., Ting, K., and Soo, C. High doses of bone morphogenetic protein 2 induce structurally abnormal bone and inflammation *in vivo*. Tissue Eng Part A **17,** 1389, 2011.
20. LeGeros, R.Z. Properties of osteoconductive biomaterials: calcium phosphates. Clin Orthop Relat Res 81, 2002.
21. Alam, M.I., Asahina, I., Ohmamiuda, K., Takahashi, K., Yokota, S., and Enomoto, S. Evaluation of ceramics composed of different hydroxyapatite to tricalcium phosphate ratios as carriers for rhBMP-2. Biomaterials **22,** 1643, 2001.
22. Seebach, C., Schultheiss, J., Wilhelm, K., Frank, J., and Henrich, D. Comparison of six bone-graft substitutes regarding to cell seeding efficiency, metabolism and growth behaviour of human mesenchymal stem cells (MSC) *in vitro*. Injury **41,** 731, 2010.
23. Goldstein, A.S., Juarez, T.M., Helmke, C.D., Gustin, M.C., and Mikos, A.G. Effect of convection on osteoblastic cell growth and function in biodegradable polymer foam scaffolds. Biomaterials **22,** 1279, 2001.
24. Niemeyer, P., Fechner, K., Milz, S., Richter, W., Suedkamp, N.P., Mehlhorn, A.T., Pearce, S., and Kasten, P. Comparison of mesenchymal stem cells from bone marrow and adipose tissue for bone regeneration in a critical size defect of the sheep tibia and the influence of platelet-rich plasma. Biomaterials **31,** 3572, 2010.
25. Na, K., Kim, S.W., Sun, B.K., Woo, D.G., Yang, H.N., Chung, H.M., and Park, K.H. Osteogenic differentiation

of rabbit mesenchymal stem cells in thermo-reversible hydrogel constructs containing hydroxyapatite and bone morphogenic protein-2 (BMP-2). Biomaterials **28,** 2631, 2007.
26. Stephan, S.J., Tholpady, S.S., Gross, B., Petrie-Aronin, C.E., Botchway, E.A., Nair, L.S., Ogle, R.C., and Park, S.S. Injectable tissue-engineered bone repair of a rat calvarial defect. Laryngoscope **120,** 895, 2010.
27. Strobel, L., Rath, S., Maier, A., Beier, J., Arkudas, A., Greil, P., Horch, R., and Kneser, U. Induction of bone formation in biphasic calcium phosphate scaffolds by bone morphogenetic protein-2 and primary osteoblasts. J Tissue Eng Regen Med **8,** 176, 2014.

Address correspondence to:
Andreas Arkudas, MD
Department of Plastic and Hand Surgery
University Hospital of Erlangen
Friedrich-Alexander-University of Erlangen-Nuernberg
Krankenhausstrasse 12
Erlangen D-91054
Germany

E-mail: andreas.arkudas@uk-erlangen.de

Received: January 11, 2014
Accepted: June 25, 2014
Online Publication Date: November 5, 2014